Desalination and Water Treatment
www.deswater.com

doi: 10.1080/19443994.2015.1005695

57 (2016) 6159–6171
March

Taylor & Francis
Taylor & Francis Group

Effect of pressure on fouling of microfiltration membranes by activated sludge

Mads Koustrup Jørgensen[a,b,*], Elmira Kujundzic[b], Alan R. Greenberg[b]

[a]*Department of Biotechnology, Chemistry and Environmental Engineering, Aalborg University, Frederik Bajers Vej 7H, Aalborg Øst DK-9220, Denmark, Tel. +45 9940 7248; Fax: +45 9635 0558; email: mkj@bio.aau.dk*
[b]*Department of Mechanical Engineering, University of Colorado Boulder, Membrane Science, Engineering and Technology (MAST) Center, 427 UCB, Boulder, CO, 80309-0427, USA, Tel. +303 492 4447; email: Elmira.Kujundzic@Colorado.EDU (E. Kujundzic), Tel. +303 492 6613; email: Alan.Greenberg@Colorado.EDU (A.R. Greenberg)*

Received 7 October 2014; Accepted 2 January 2015

ABSTRACT

The effect of pressure on fouling layers formed by diluted activated sludge was studied in real time with ultrasonic reflectometry by fouling microfiltration membranes for 300 min at constant pressure (0.15 bar (15 kPa) and 0.25 bar (25 kPa)), as well as by performing a series of pressure-step experiments in which the pressure was instantaneously increased from 0.15 to 0.25 bar. For the constant pressure experiments, the change in ultrasonic signal amplitude was inversely proportional to the degree of fouling as represented by changes in permeability and the amount of deposited material. This finding was verified by a series of replicated filtration experiments of 15, 30, and 60-min duration at 0.15 bar, which indicated a statistically significant correlation between the degree of fouling (quantified by permeability loss and post-mortem characterization metrics) and ultrasonic amplitude change. Diluted activated sludge filtrations at varying pressures revealed that there is less ultrasonic amplitude reduction at higher pressure where the resistance of the fouling layer is higher. This finding reflects the formation of a hydrated fouling deposit that serves as an impedance matching layer with the water-filled membrane that produces lower reflection at lower pressure. Thus, the fouling layer is thought to be less hydrated and denser at higher pressures, which confirms that the fouling layer is a compressible structure. Given that fouling layer mechanical behavior may well influence membrane filtration performance, it may be possible to improve membrane bioreactor filtration by engineering fouling layer compressibility.

Keywords: Fouling; Activated sludge; Microfiltration; Cake compression; Ultrasonic reflectometry

1. Introduction

Membrane fouling remains the major factor limiting the efficiency of membrane filtration systems particularly for membrane bioreactors (MBRs), where fouling due to sludge filtration almost always occurs. MBR fouling has been studied extensively as a function of different operational parameters including the physical and chemical characteristics of the feed suspension, membrane module hydrodynamics, and membrane type [1–3].

*Corresponding author.

Fouling reduces filtration performance by adding an additional resistance to filtration, R_f, described by the Darcy equation (Eq. (1)):

$$J = \frac{TMP}{\mu(R_m + R_f)} \quad (1)$$

where J is the permeate flux [$m^3\ m^{-2}\ s^{-1}$], TMP is the transmembrane pressure [Pa], μ is the dynamic viscosity of water [Pa s], and R_m is the inherent membrane resistance [m^{-1}]. Increasing resistance related to the development of fouling leads to a decrease in permeate production at constant pressure filtration or an increase in pressure at constant flux operation. Membranes in MBR systems are affected by pore blocking, adsorption, cake formation, biofilm, or gel formation as well as scaling from foulants ranging from salts, macromolecules, colloids, sludge flocs, and microorganisms [1–3]. Of these fouling mechanisms, cake layer formation has been shown to be the most dominant [4].

The resistance of membrane sludge-cake layers, R_c [m^{-1}], can be calculated from the following equation (Eq. (2)) [4,5]:

$$R_c = \alpha_c \cdot \omega_c \quad (2)$$

where α_c is the specific cake resistance representing the characteristics of the sludge and the cake layer [m kg^{-1}], and ω_c is the mass of cake layer per surface area [kg m^{-2}]. For membrane filtration, it is well established that the cake layers formed on membrane surfaces are pressure dependent [6,7]. Increasing operating pressure gives a higher specific cake resistance due to cake compression, whereas decreasing the pressure yields a lower specific cake resistance due to cake swelling [5].

For membrane filtration of activated sludge in MBR systems, the compressibility of fouling layers has been described in only a few studies. Teychene et al. [8] determined that filtration performance can be optimized by modifying the compressibility of the fouling layers in MBR supernatant filtration with fine particle addition. Effects of cake compressibility are also reported in Zhang et al. [9], where the compressibility of fouling layers is used to describe the TMP jump at constant flux filtration. In addition, a dynamic model has been used for membrane bioreactor fouling, incorporating the influence of pressure on the specific cake resistance [10,11].

Jørgensen et al. [12] and Bugge et al. [13] have shown that the compressibility of the cake layers formed in MBR filtration has a significant influence on filtration resistance, which should be accounted for during operation. They report that the fouling resistance in short-term MBR filtration is best represented as a combination of cake layer formation and compression, and that the change in permeate flux during pressure-step experiments could be simulated from simple models describing these two mechanisms. However, it is difficult to isolate the effects of cake layer formation and cake compression from TMP and permeate flux data alone, since a change in pressure might induce cake formation as well as compression with a resulting increase in the specific resistance of the cake layer. Thus, there is a strong rationale for a more quantitative characterization of such cake layers in order to provide an improved understanding of cake layer behavior and its effect on membrane performance.

The demand for more direct methods to study the development of membrane fouling in MBR systems and in membrane filtration processes in general has led to an increasing number of studies that describe the development of techniques that can monitor the initiation of fouling on membranes noninvasively and in real time [14]. Fouling monitoring methods are often grouped into optical and nonoptical techniques. A significant disadvantage of the optical techniques is that they require an "optical window" and are, therefore, unable to monitor fouling on membranes in a turbid feed-stream system [14]. Therefore, optical methods are not a realistic option for direct online, real-time monitoring of fouling in many membrane processes including MBR systems. In contrast, ultrasonic reflectometry (UR) is able to detect fouling noninvasively in a wide range of membrane processes and is not significantly affected by the turbidity of the feed stream [15–22].

As reported in a recent review [22], UR has successfully been used to quantify and determine the onset of fouling caused by inorganic and organic foulants. The amount of fouling is generally quantified by post-mortem analysis of the fouled membranes via gravimetric measurements and/or scanning electron microscopy (SEM). Post-mortem quantification of the degree of fouling can then be related to systematic changes in the ultrasonic spectra. In a recent study by Lu et al. the onset of calcium sulfate scaling of a reverse osmosis membrane was detected via a reduction in the amplitude of the signal reflected from the membrane [15]. Li et al. used UR to detect yeast fouling of a hollow fiber membrane [16], and a study by Kujundzic et al. reported that the amplitude of the reflected ultrasonic wave increased as the microfiltration (MF) membrane pores were blocked due to protein fouling [17]. In another study by Kujundzic et al. biofilm growth on MF membranes submerged in a

biological reactor was monitored using UR. Here, the ultrasonic metric employed was total reflected power, which corresponded well with increasing amounts of biofilm associated with the membrane as expressed in terms of exocellular polysaccharide (EPS) concentration [18]. Other researchers have reported that the thickness of fouling layers formed by filtration of brown surface water could be determined from the change in ultrasonic amplitude via post-mortem analysis such as SEM that linked the change in ultrasonic amplitude with the degree of fouling [19]. Fouling layers formed by oily sludge have also been monitored with UR [20,21], but there are currently no literature reports describing UR monitoring of membrane fouling with municipal wastewater sludge or activated sludge. Furthermore, there is a lack of information in the literature regarding direct monitoring of the viscoelastic response of activated sludge fouling layers, although such behavior has been shown to have a significant impact on filtration [7–13].

Given the success of UR in monitoring inorganic/organic fouling and biofouling of membranes in different module configurations, the specific objectives of this study are to adapt UR for monitoring membrane fouling from municipal wastewater sludge and to combine UR with pressure-step filtrations to quantify the effect of the operating pressure on the cake structure.

Since the use of concentrated activated sludge would cause very rapid and extensive fouling, this study utilizes diluted activated sludge in order to obtain improved resolution for monitoring early-stage fouling layer formation, which can be correlated with systematic changes in the ultrasonic signals. The effect of operating pressure is studied by monitoring the ultrasonic amplitude and hydraulic resistance to filtration at pressures of 0.15 bar (15 kPa) and 0.25 bar (25 kPa). The dynamics of cake compression and swelling are studied by introducing pressure-step experiments, where pressure is systematically stepped between 0.15 and 0.25 bar at specified intervals, and ultrasonic amplitude and hydraulic resistance are monitored.

Further, the study considers the relationship between the ultrasonic amplitude and degree of fouling by means of a time-series filtration approach whereby the ultrasonic signals are compared to the degree of fouling obtained after exposure during controlled intervals of sludge filtration at 0.15 bar. The degree of fouling is quantified via post-mortem characterization that includes gravimetric analysis, measurement of protein concentration, and changes in reflected light intensity during optical examination of the membrane surface. With this comprehensive experimental approach, the real-time changes in the amplitude of the ultrasonic wave reflected from the membrane/feed interface during fouling can be correlated with the overall degree of fouling determined from independent real-time and post-mortem metrics.

2. Methodology

2.1. Membrane preparation

A polyvinylidene fluoride (PVDF) membrane from Alfa Laval (Batch No. 112091-04, Alfa Laval-MFP2, Denmark) was selected for the study, as it is commonly used for activated sludge filtration in MBR systems. This membrane has a polypropylene support and a PVDF active layer with a nominal pore size of 0.2 μm. Membranes for filtration were cut from the roll and soaked in 50% (w/w) ethanol for at least 6 h to remove the glycol present as a preservative. Before installing membranes in the filtration system, they were further rinsed with deionized (DI) water to remove any ethanol residue.

2.2. Cross-flow filtration system integrated with on-line ultrasonic instrumentation

The cross-flow filtration system with integrated online ultrasonic instrumentation is illustrated in Fig. 1.

A tank with 6 L of feed solution was connected to a pump (MK 300 series, Fluid-o-Tech, Italy), which was powered by a motor (model M2VA56B-2, ABB Motors, Switzerland) that introduced feed solution into the polysulfone cross-flow filtration cell and pressurized the system. The feed tank was aerated at a rate of 5 L/min, and the operating pressure was measured via a pressure transducer (model MBS4010, Danfoss, Denmark). The feed chamber of the cross-flow cell had a length of 250 mm, width of 120 mm, and height of 5 mm, giving an active membrane surface area of 0.03 m^2. The other half of the cell contained a porous polyethylene (PE) plate that served as a support for the membrane. The permeate that passes through the membrane and PE plate was measured via a flow meter (model 105 Flo-Sen, McMillan, TX, USA); permeate was returned to the feed tank during DI water filtration. During low-flow conditions, i.e. fouling experiments, the permeate flow rate was determined by measuring the mass of permeate collected over a fixed time period in a beaker placed on a balance (model PB3002-L, Mettler-Toledo, OH, USA).

Retentate from the cell was recirculated, and a constant cross-flow was maintained with a pump (model TMFR1, Fluid-O-Tech, Italy) and a flow meter (model Flo-Meter 114, McMillan, TX, USA). Additional retentate was channeled back to the feed container, and

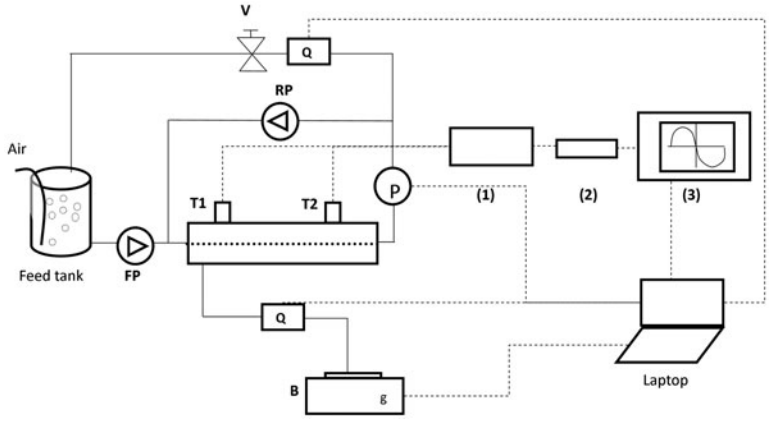

Fig. 1. Schematic illustration of the cross-flow filtration system with two ultrasonic transducers (T1 and T2) connected to the external surface of the cross-flow filtration cell: (1) multiplexer; (2) pulser/receiver; (3) oscilloscope; FP: feed pump; RP: recirculation pump; V: valve; Q: flow meter; P: pressure transducer; and B: balance.

was controlled with a needle valve (model SS-1RM4-S4-A, Swagelok, OH, USA).

Two 10-MHz ultrasonic transducers (model V111, Panametrics, MA, USA) were mounted on the top plate of the feed chamber. The ultrasonic transducers were located 7 cm from the feed inlet (upstream) and 7 cm from the retentate outlet (downstream). Each transducer was connected with a custom-built multiplexer that controlled the order in which signals from the ultrasonic transducers were transmitted to the pulser/receiver (model 5072 PR, Panametrics, MA, USA) and oscilloscope (model TDS3052, Tektronix, TX, USA). A custom-assembled LabView program (National Instruments, TX, USA) recorded the spectra from the two ultrasonic transducers every 10 min during membrane compaction and every 2 min during the fouling phase.

The pressure transducer and flow meter were connected to an I/O analog–digital signal converter (USB-1208LS, Measurement Computing, MA, USA) that was linked to a laboratory PC. In addition, the balance was connected to the PC via a serial RS232 communication cable. The mass, pressure, and permeate flow rates were recorded at 1-s intervals and acquired by a custom-built Delphi program (Borland Software Corporation, CA, USA).

The temperature in the feed tank was monitored via a temperature sensor (model #UA-001-64, HOBO, Onset Computer Corporation, MA, USA) every 10 min. The temperature of the feed measured over the course of the experiments was 25.6 ± 0.5°C.

2.3. Physical and chemical analysis of sludge samples

Sludge samples were collected from the Boulder Wastewater Treatment Facility, Boulder, CO, USA. Since the sludge samples were collected over a period of a four months, they were analyzed to ensure that there were no systematic changes in sludge characteristics that might inadvertently affect the fouling experiments. The conductivity and pH of the sludge were measured with two sensors (model ECTestr11+ and pHTestr 20 Eutech Instruments, IL, USA). The concentration of total suspended solids (TSS) in the sludge was determined by filtering three subsamples per single sludge sample. The volume of the sludge subsamples and the mass of dry filter paper (47-mm, 0.6 μm, GA-55, Advantec, Japan) was determined prior to vacuum filtration (model AG245, Mettler Toledo, MI, USA). After filtration, the filter paper was dried in a laboratory oven (Isotemp Standard Lab Oven, Fisher Scientific, PA, USA) at 105°C for 12 h and reweighed. The total suspended solids concentration was calculated as the difference between the weight of the filter paper before and after filtration. The particle-size distribution was determined using a particle sizer (Accusizer 780 Optical Particle Sizer, Nicomp International, FL, USA). Additionally, the concentration of dissolved EPS was determined in three subsamples of each sludge sample by measuring the concentration of proteins and humic acids using the modified Lowry method [23,24], and the concentration of sugars was obtained using a modified Anthrone method [25,26] in the supernatant of the centrifuged sludge samples. The protocol utilized bovine serum albumin (BSA), humic acid, and glucose as standards.

2.4. Cross-flow cell experiments

Polymeric membranes have pressure-sensitive structures that undergo compression (compaction)

during filtration startup, which produces a change in the ultrasonic signal reflected from the membrane [17,27]. Therefore, all fouling experiments were conducted only after a 15-h setting phase in DI water during which measurable membrane compaction was completed.

Before sludge was added to the feed tank to obtain a sludge concentration of 0.2 g/L, the conductivity of the DI water was adjusted to the same conductivity as that of the sludge. Water conductivity was set in this manner to prevent deflocculation of the sludge flocs. Filtration was performed at either 0.15 bar (15 kPa) or 0.25 bar (25 kPa) at a cross-flow rate of 2.45 L/min corresponding to a cross-flow velocity of 0.085 m/s and laminar flow ($Re = 137$).

2.4.1. Full-fouling experiments

The goal of the full-fouling experiments is to observe the effect of the sludge on real-time membrane performance metrics at pressures of 0.15 and 0.25 bar, respectively, over a time period that is sufficient for extensive fouling to occur. Based upon the reduction in the permeate flow rate and UR metrics as well as the post-mortem results from gravimetric and microscopic analysis, significant membrane fouling occurred after 300 min of exposure to the sludge. These experiments provided a useful reference point for establishing more limited exposures so that the real-time results could be more meaningfully correlated with the post-mortem metrics. Filtrations were repeated three times, and ultrasonic spectra from the upstream and downstream transducers were collected for each experiment.

2.4.2. Stepped-pressure experiments

The effect of pressure on sludge fouling was studied at two different pressures: 0.15 and 0.25 bar. The filtration pressure may influence the initial membrane structure since the polymeric membrane can evidence viscoelastic behavior. Increasing the pressure can lead to additional time-based deformation (creep) of the membrane, whereas releasing pressure leads to membrane recovery [27]. Since compaction of the membrane changes the ultrasonic reflection characteristics from the membrane, reference levels for the membrane amplitude were obtained at the completion of the DI water setting phase at the given pressure.

To provide additional insight regarding fouling dynamics, stepped-pressure experiments were performed whereby the pressure was systematically varied between 0.15 and 0.25 bar in five cycles. These experiments started with Cycle A (0.15 bar). After 30 min, the pressure was increased to 0.25 bar (Step 1) to start Cycle B. After an additional 30 min, the pressure was decreased to 0.15 bar (Step 2) for a 60-min filtration (Cycle C). This was followed by stepping the pressure (Step 3) 0.25 bar for 30 min (Cycle D) before decreasing the pressure to 0.15 bar (Step 4) for another 30 min at which point the filtration experiment was terminated (Cycle E). For these individual phases with filtration at either 0.15 or 0.25 bar, reference periods with DI water filtration at 0.15 and 0.25 bar, respectively, were used as a baseline. The stepped-pressure experiments were repeated three times with ultrasonic spectra obtained from both the upstream and downstream transducers.

The fouling layer resistance, R_f, was calculated from Eq. (1) to determine the extent of fouling layer compression at the higher pressures. For this calculation, a combined membrane and system resistance of $R_m = 9.6 \times 10^{11}\ m^{-1}$ was used, as determined from DI water filtration.

2.4.3. Time-series experiments

To quantify the influence of fouling on the ultrasonic response, experiments with varying filtration times: 15, 30, and 60 min were performed at 0.15 bar. The ultrasonic data were compared with changes in permeate flux over the fouling period and to the post-mortem characteristics of the fouled membranes. After fouling the membrane over the desired interval, filtration was terminated, and the membrane was removed from the cell. Membrane coupons were sectioned from the regions underneath the upstream and the downstream ultrasonic transducers for post-mortem characterization, which is further described in Section 2.5. All experiments were repeated three times, and ultrasonic spectra from the upstream and downstream transducers were collected from each experiment.

2.5. Post-mortem characterization

Membrane coupons were cut from the fouled membranes immediately after the time-series experiments. The membrane was removed from the filtration cell, and coupons (2.54 × 2.54 cm, surface area: 6.45 cm^2) were sectioned with a punch from the regions of the membrane that were directly beneath the ultrasonic transducers. The coupons were analyzed to quantify the mass of foulant associated with each region of the membrane.

2.5.1. Optical examination

Membrane coupons dried in an oven (Isotemp Standard Lab Oven, Fisher Scientific, PA, USA) at

105˚C for at least 12 h were analyzed with an optical microscope (model 6000 Micromanipulator, NV, USA) at 20X magnification. The coupons included sections from the membranes fouled for 15, 30, and 60 min, and nonfouled membranes. The microscope was connected to a PC equipped with commercial software (Infinity Capture Software 21-c, Lumenera Corporation, Canada) to obtain images of the membrane samples. The intensity of the image was quantified with ImageJ software (National Institutes of Health, MD, USA), and average gray brightness values were determined using identical microscope settings for each membrane sample image. The intensity values were normalized with the gray brightness level of a DI water-filtrated membrane.

2.5.2. Gravimetric analysis

The amount of material deposited on the membrane coupons from the time-series experiments and nonfouled (virgin) membranes used as a reference was determined by chemical cleaning. Dry membrane coupons were weighed (model AG245, Mettler Toledo, MI, USA) and then cleaned with a 0.3%w/w sodium hypochlorite solution (diluted from hypochlorite aqueous solution, reagent grade solution, Alfa Aesar, China). The amount of foulant was then calculated from the weight loss (in grams) due to chemical cleaning divided by the membrane surface area.

2.5.3. Biochemical assay

The concentration of protein on two membrane coupons, one from the upstream and downstream ultrasonic transducer for filtration experiments at 15, 30, and 60 min was determined and compared to that from a virgin membrane, i.e. one not exposed to sludge fouling.

Water-soluble proteins were eluted from the membrane coupons using the following procedure. Membrane coupons were aseptically placed in 50-mL plastic test tubes. A total of 15 mL of ultrapure sterile water was added, and the resulting solution was sonicated on ice for 1 h. The eluent was then analyzed for protein content using a bicinchoninic acid (BCA) kit (Pierce, Rockford, IL) and a BSA standard calibrator. Colorimetric results were obtained by reading absorbance at 562 nm using a spectrophotometer (model DR/2010, Hach, CO, USA).

2.6. Ultrasonic spectrum analysis

The arrival time, t, of a wave traveling from the ultrasonic transducer and back again after being reflected from the membrane/feed interface was calculated from Eq. (3):

$$t = 2l/c \tag{3}$$

where l is the distance to the reflecting interface, and c is the speed of sound in the given medium (polysulfone: 2,260 m/s; water: 1,493 m/s). Note that the travel distance is twice the path length from the ultrasonic transducer to the reflecting interface, as the ultrasonic wave travels to the interface region and back. This equation was used to calculate the travel time for an ultrasonic wave through a 19-mm polysulfone plate and a 5-mm water channel at a temperature of 25.6˚C to determine the expected arrival time of the ultrasonic wave reflected from the cell wall/feed interface and the wave reflected from the membrane/feed interface.

The arrival times for the membrane/feed and cell wall/feed interfaces were calculated to be 23.5 and 16.8 μs, respectively. From these expected values, the waves reflected from the cell wall/feed and the membrane/feed interfaces were identified in the ultrasonic spectrum recorded by the oscilloscope.

Fouling can lead to either an increase [18] or reduction [17] of the amplitude of the membrane reflected wave depending upon the characteristics of the fouling layer, but in either case the change in ultrasonic amplitude can be correlated to the degree of fouling. The magnitude of the amplitude for a reflected wave at time, t, is simply obtained as a peak height, i.e. the difference between the maximum amplitude, A_{max}, and the minimum amplitude, A_{min} (Fig. 2) [15].

The peak height was normalized using the first amplitude value measured for DI water or sludge filtration. To describe the change in amplitude when the membrane was fouled, the initial normalized amplitude at the start of the fouling phase was used as a baseline value. The percent reduction in amplitude at time t, A_r, is then calculated per Eq. (4):

$$A_r = 100\% \times \frac{A_0 - A_t}{A_0} \tag{4}$$

where A_0 is the initial normalized amplitude and A_t is the normalized amplitude at time t. The change in amplitude was used as the ultrasonic metric for quantifying the extent of fouling.

2.7. Statistical evaluation

Standard statistical analysis techniques were utilized to rigorously assess differences and correlations

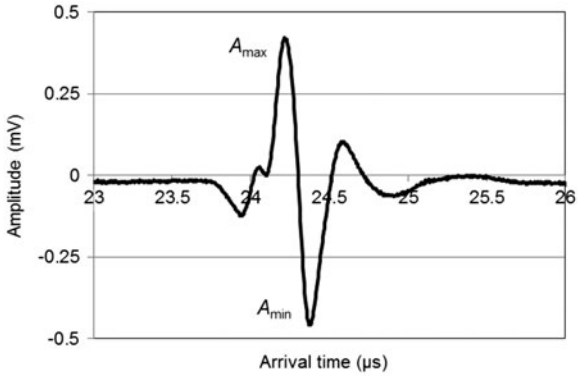

Fig. 2. Representative waveform showing ultrasonic amplitude as a function of arrival time for membrane compaction during filtration with DI water. A_{max} and A_{min} are the maximum and minimum ultrasonic amplitude, respectively, and are used to calculate the overall real-time ultrasonic signal amplitude.

among the real-time and ultrasonic responses during the time series and pressure-step experiments [28]. The techniques employed to determine statistical significance ($\alpha \leq 0.05$) included the Student's *t*-test and analysis of variance.

3. Results and discussion

3.1. Physical and chemical characteristics of sludge samples

The mean values for TSS, conductivity, pH, particle diameter for the activated sludge, and sugar, protein, and humic acid concentrations collected from the Boulder Wastewater Treatment Facility are given in Table 1.

Analysis of the sludge identified no significant changes in the physical and chemical properties of the sludge over the sampling period. Therefore, it is reasonable to compare sludge filtration results during the course of the study.

3.2. Full-fouling experiments

Representative results for the permeate flux during filtration with DI water and during the subsequent filtration of sludge are presented in Fig. 3. During DI water filtration (Fig. 3, top), the flux evidences a modest decrease (3–5%) at each pressure due to membrane compaction. As expected, the initial flux is higher at 0.25 bar, but the rate of decrease at each pressure is quite similar. The introduction of sludge (Fig. 3, bottom) rapidly results in a more pronounced flux decline (55% at 0.15 bar and 61% at 0.25 bar). The initial flux at 0.25 bar is higher than that at 0.15 bar due to the higher driving force, but the rate of decrease at 0.25 bar is somewhat higher such that the flux values are almost the same after 300 min.

When sludge was introduced, a decrease in ultrasonic amplitude from the membrane-feed interface was observed, but no separate UR signal for the fouling layer appeared in the waveform. The reduction of ultrasonic amplitude during filtration experiments was calculated using Eq. (4). The percentage change in amplitude at 30-min intervals for 5-h filtration experiments at 0.15 and 0.25 bar using diluted activated sludge is presented in Fig. 4 (top). Each datum represents the mean amplitude reduction (%) from six values (three experiments with two transducers). Results show that the amplitude decreases with time at a similar rate at each pressure. In Fig. 4 (bottom), the fouling resistance is plotted against the percentage decrease in amplitude for representative filtrations at 0.15 and 0.25 bar. This shows that as the amplitude decreases throughout the 300-min filtration experiments, the fouling resistance increases linearly, which suggests that the amplitude decrease can be associated to the degree of fouling. Analysis indicates that there is a statistically significant ($p < 0.05$) linear correlation between the increase in fouling resistance and the reduction in amplitude at each pressure. Further, the change in amplitude over time was analyzed using the approach presented in Lu et al. [15]. The analysis indicated that the induction times for the ultrasonic amplitude to respond to membrane cake formation were 1.57 ± 0.79 min and 11.28 ± 3.77 min for the filtrations at 0.15 and 0.25 bar, respectively, although the corresponding loss of permeability was instantaneous at each pressure.

The observed decrease in the ultrasonic amplitude from the membrane/feed interface has been

Table 1
Characteristics of activated sludge from the Boulder Wastewater Treatment Facility

Parameter	TSS (g/L)	Conductivity (μS/cm)	pH	Particle diameter (μm)	Sugars (mg/L)	Proteins (mg/L)	Humic acids (mg/L)
Mean ± SD*	2.65 ± 0.16	771 ± 62	6.67 ± 0.18	156.2 ± 13.2	22 ± 4	73 ± 17	199 ± 40

*SD: standard deviation.

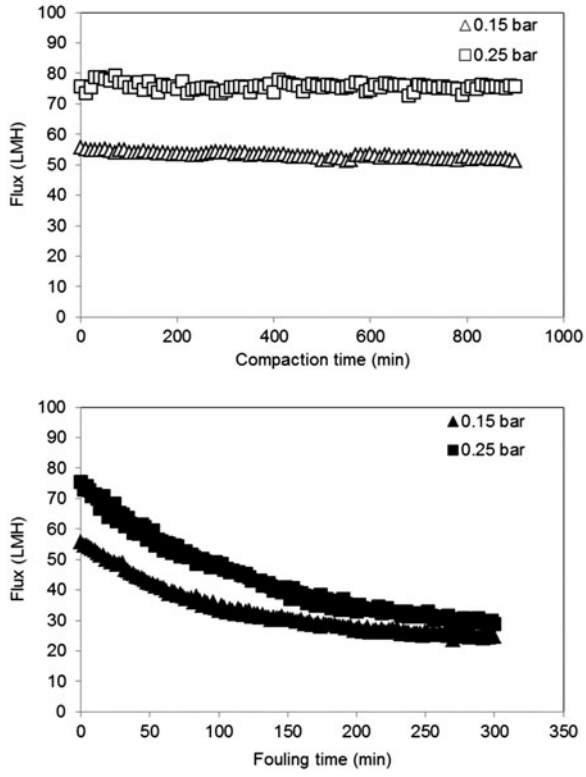

Fig. 3. Representative results showing permeate flux as a function of time during the compaction phase with DI water (top) and during the subsequent filtration of diluted activated sludge (bottom) at pressures of 0.15 and 0.25 bar.

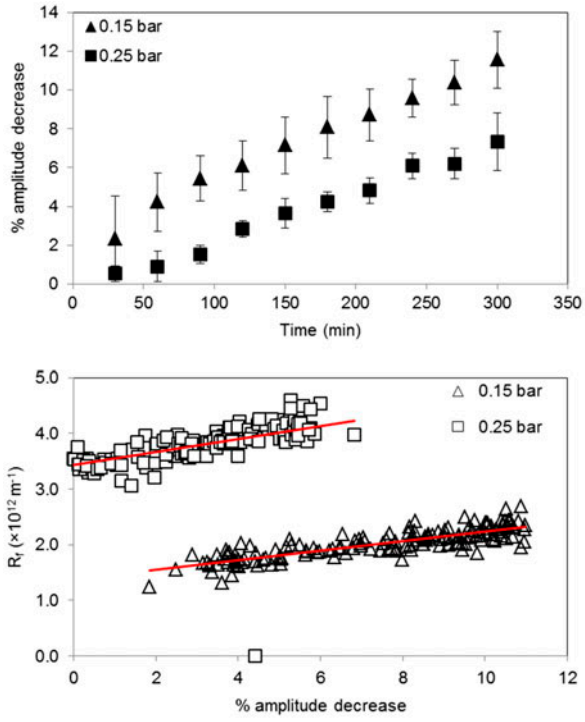

Fig. 4. Representative results showing the influence of pressure on ultrasonic amplitude as a function of exposure time (top) and fouling resistance vs. % amplitude decrease (bottom) throughout diluted activated sludge filtration experiments at pressures of 0.15 and 0.25 bar. Error bars (top) represent the standard deviation; linear correlation lines (bottom) are statistically significant.

previously reported for membrane scaling and biofouling [15,18] although the physics is different. For the initial stages of calcium sulfate scaling, amplitude reduction is primarily a result of scattering from the randomly oriented platelets that comprise the salt crystal rosettes [29,30]. In contrast, the reduction of amplitude by formation of an organic fouling layer is explained by the fact that the fouling layer serves as an impedance matching layer, which reduces the intensity of the reflected wave via absorption [31]. In the subject experiments, amplitude reduction was statistically greater at the lower pressure even though fouling resistance after 300 min was more pronounced with filtration at 0.25 bar (Fig. 4, bottom). This phenomenon is further explored in the pressure-stepping experiments in Section 3.3.

3.3. Stepped-pressure experiments

A set of stepped-pressure experiments was conducted during which the flux and fouling resistance as well as ultrasonic amplitude were measured. These experiments consisted of five cycles during which the pressure was systematically stepped between 0.15 and 0.25 bar. Fig. 5 shows representative plots of flux, fouling resistance, and amplitude over time in the stepped-pressure experiments. Fig. 5 (top) shows that the flux decreases during each cycle, but evidences either rapid recovery or rapid decline as the pressure is decreased or increased, respectively. Fouling resistance increases considerably during the first three cycles (A–C), and the effect of the pressure changes on resistance and flux is significant. An even larger increase in resistance occurs when the pressure is increased from 0.15 to 0.25 bar in Step 3, but the increase in flux is more modest than at 0.15 bar with a continued increase in resistance and decrease in flux during this cycle (D). With the final decrease in pressure (Step 4), the resistance initially declines and remains essentially constant, while the flux again initially decreases but quickly reaches a constant value.

The decrease in amplitude (Fig. 5, bottom) is calculated from a reference amplitude recorded for DI water at the given pressure (either 0.15 or 0.25 bar) prior to membrane fouling. The amplitude decreases during Cycles A and C but remains relatively

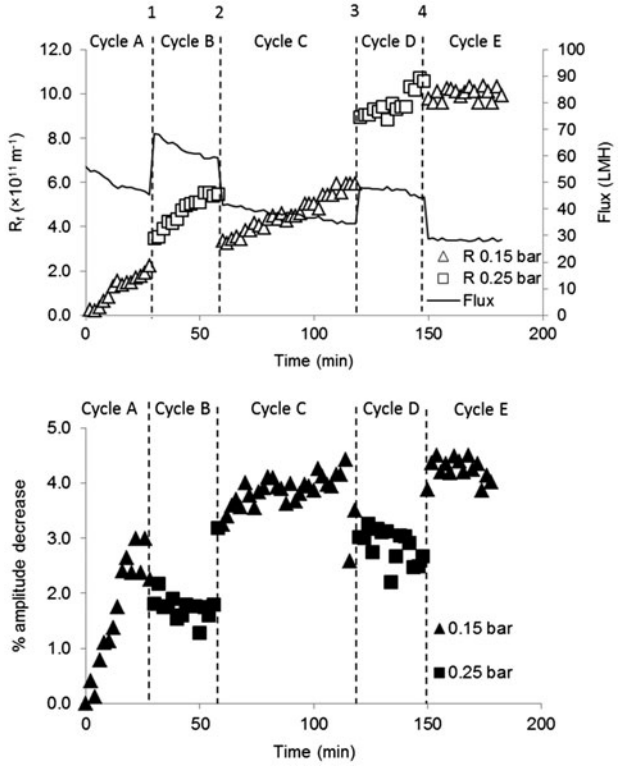

Fig. 5. Representative results from a five-cycle pressure-step experiment with diluted activated sludge. The pressure was altered in a controlled series of steps (dashed lines 1–4) between different filtration cycles at: Cycle A: 0.15 bar for 30 min; Cycle B: 0.25 bar for 30 min; Cycle C: 0.15 bar for 60 min; Cycle D: 0.25 bar for 30 min; and Cycle E: 0.15 bar for 30 min. Top: Permeate flux and fouling resistance; Bottom: ultrasonic amplitude decrease.

unchanged during Cycle E, inversely following the trends in resistance. The response to the step to higher pressure that initiates Cycles B and D is a slight recovery (less of a decrease) during the cycles. Interestingly, the signal amplitude appears rather sensitive to the relatively small decreases in pressure at Steps 2 and 4.

The stepped-pressure experiments confirm the observations from the full-fouling experiments at 0.15 and 0.25 bar (Fig. 4) that there is a greater reduction in amplitude at lower pressure. The stepped-pressure experiments also confirm the pressure dependence of the fouling layer hydraulic resistance, with higher resistance at higher pressure at least through the first four cycles.

The increase in fouling resistance with increasing pressure (Fig. 5) could be explained by the compressibility of the fouling layer. In several studies, it has been reported that organic fouling layers are compressible and that the compression of fouling layers leads to higher specific resistances for filtration [6,7]. This has also been reported to apply to membrane deposits of sludge compounds [12]. As the pressure increases, the fouling layer is compacted and becomes denser; as the pressure decreases, the fouling layer swells and becomes less compact with a lower resistance, depending on the degree of reversibility of compression [32]. This hypothesis is consistent with the observation that sludge fouling layers behave as viscoelastic cakes that are compressed at higher pressures and then swell when the pressure is reduced, but not necessarily in a completely reversible manner [12,32]. Such fouling layer behavior could be consistent with the greater degree of membrane amplitude decrease observed at lower pressure. As indicated in reference [33], the amplitude should not be significantly affected by a small change in pressure unless the material properties of the media are altered. A water-swollen cake layer will more closely reflect the ultrasonic characteristics of the water-swollen membrane, i.e. there is a greater degree of impedance matching and hence enhanced attenuation. Therefore, reduction of the signal amplitude would be expected as a more hydrated cake layer is formed on the membrane surface. In addition, the increased thickness of the swollen layer could also contribute to increased signal attenuation via energy absorption. This ultrasonic amplitude response could be rather different if the predominant fouling mechanism were pore blocking rather than cake formation. As pressure is stepped to a higher value, the fouling resistance and ultrasonic amplitude increase (less reduction). These responses are also consistent with cake compression. The rapid reclamation of ultrasonic amplitude reduction as the pressure is lowered combined with the decrease in fouling resistance support the reversibility of cake compression such that the cake swells as the pressure is reduced. Although resistance decreased when the pressure was reduced, the flux also declined due to the lower driving force for filtration. The decrease in resistance when lowering pressure between Cycles B and C suggests a high degree of compression reversibility, i.e. the cake swells and returns to its uncompressed structure. However, the decline in resistance between Cycles D and E suggests that compression is not entirely reversible as the previous level is not attained. Thus, this response may well be affected by accelerated deposition of foulants during Cycle D, which will not be removed when the pressure is lowered. The influence of pressure on the fouling layer impedance properties is also observed by the difference in amplitude-determined induction time at different pressures, as reported in Section 3.2. At 0.15 bar filtration, the induction time is shorter even though there is less fouling at the lower pressure. This could be explained

by the less compressed fouling layer that reduces the signal amplitude to a greater degree than the compressed fouling layer obtained at 0.25 bar. Hence, the detection of the onset of fouling by signal amplitude reduction appears more sensitive at the lower pressure.

3.4. Time-series experiments

To verify that the change in ultrasonic amplitude at constant pressure filtration is related to the degree of fouling, time-series experiments were carried out together with post-mortem characterizations of fouled membrane coupons. The reduction of ultrasonic amplitude (Eq. (4)) was calculated from three experiments performed at three selected fouling times: 15, 30, and 60 min using data from the upstream and downstream ultrasonic transducers. Results for time-series experiments conducted at 0.15 bar are presented in Fig. 6. Similar to the results obtained in the full-fouling experiments, analysis of the time-series data indicates that there is a systematic decrease in the amplitude with an increase in fouling time; however, the differences between the two transducers are not statistically significant (Fig. 6, top) ($p > 0.05$). The lack of a significant difference in the amplitude response from the two transducers is not surprising given that the short length of the feed chamber (250 mm) does not support the development of a fouling gradient from the upstream to the downstream location. Therefore, it can be assumed that fouling was distributed relatively uniformly over the membrane surface. Fig. 6 (middle) shows the systematic decrease in flux with an increase in filtration time. The permeate flux and UR responses are quite similar, although the magnitude of the flux decrease is greater than that observed for the ultrasonic amplitude. This is expected given that the former is an average metric, whereas the latter is effectively a point measurement [22]. As indicated in Fig. 6 (bottom), the correlation between the flux and ultrasonic amplitude responses is linear and statistically significant ($p < 0.05$). This finding, in combination with the results in Fig. 4 (bottom), strengthens the assertion that at constant pressure there is a consistent inverse relationship between the degree of sludge fouling and the change in ultrasonic amplitude.

When membranes fouled for 0, 15, 30, and 60 min were analyzed via optical microscopy, it was observed that the membranes exhibited uniform fouling over the entire surface with no indication of patchiness. This observation is consistent with the previously noted lack of a significant difference between the responses of the upstream and downstream transducer. The normalized

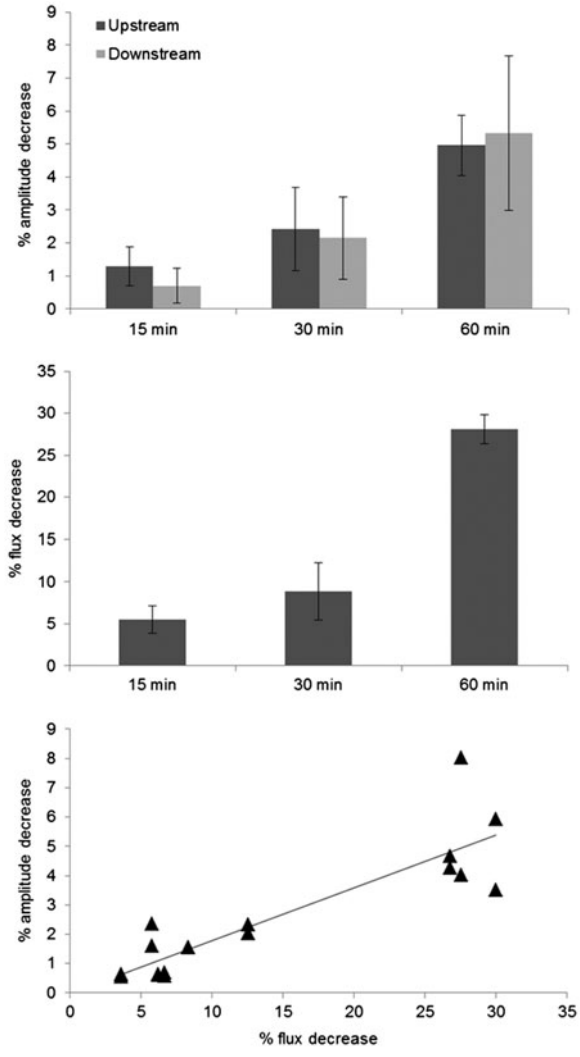

Fig. 6. Results from time-series experiments at a pressure of 0.15 bar during exposure to diluted activated sludge: reduction of ultrasonic signal amplitude for upstream (black) and downstream (gray) ultrasonic transducer (top); corresponding reduction in flux (middle); and correlation between ultrasonic amplitude and permeate flux responses (bottom). Error bars represent the standard deviation.

gray brightness values determined via image analysis as well as the amount of foulant removed by chemical cleaning are presented in Table 2. Membranes not exposed to sludge but only to DI water are labeled as "0". The results indicate a systematic decrease in brightness with an increase in filtration time although the data are not statistically significant ($p = 0.078$) likely due to the combination of small sample size and relatively large standard deviation at the 15-min fouling time.

The gravimetric data in Table 2 show that the mass of the reference (virgin) samples was unchanged after

Table 2
Post-mortem analysis of membrane coupons fouled with activated sludge in time-series experiments at 0.15 bar

Fouling time (min)	Normalized gray brightness ± SD (%)	Mass of removed foulant ± SD (μg/cm^2)	Protein concentration ± SD (μg/m^2)	Flux decrease ± SD (%)	Amplitude decrease ± SD (%)
0	100 ± 1	0.00 ± 0.02	Below detection limit		
15	62 ± 20	0.11 ± 0.04	171 ± 0	5.5 ± 1.5	0.6 ± 0.1
30	49 ± 14	0.17 ± 0.02	177 ± 2	8.9 ± 3.1	1.9 ± 0.4
60	30 ± 6	0.31 ± 0.04	183 ± 0	28.1 ± 1.5	5.1 ± 1.7

SD: standard deviation.

chemical cleaning, whereas the mass removed from the fouled membranes during chemical cleaning increases with filtration time. The assumption that the mass loss during chemical cleaning can be directly linked to the amount of fouling is reasonable under the assumption that all of the fouling is removed. Note that the method utilized is that employed commercially for removing organic fouling, which is the main type of fouling for activated sludge filtration. However, this method may underestimate the total mass of fouling since it does not include any fouling removed when the filtration system is emptied and the membrane removed. In addition, relaxation can occur as filtration is terminated, which can remove some sludge fouling in a matter of minutes [12]. Therefore, only fouling consisting of adsorbed foulants, a strongly adhered cake, and blocked pores are accounted for using this technique. Nonetheless, for the short-term experiments used in this study, the amount of unaccounted fouling mass should be small and proportional to the total amount of fouling. Finally, results from Table 2 indicate that the protein concentration increases systematically from a very low level (below the detection limit) for a virgin membrane to a value of 183 ± 0 μg/m^2 for the sample fouled for 60 min. Since both the foulant mass and protein concentrations were statistically significant with respect to the duration of the time-series fouling experiments ($p < 0.05$), the mass of foulant removed as well as the protein concentration are taken as independent measures that are proportional to the degree of membrane fouling. In summary, the post-mortem metrics and permeate flux decline values in Table 2 confirm that an increase in fouling results in a systematic decrease in ultrasonic signal amplitude.

3.5. Potential of the methodology

The results of this work support the findings reported in other studies regarding the viscoelastic nature of the fouling layers formed by activated sludge [12,13]. Therefore, the compressibility of fouling layers formed by wastewater sludge, e.g. in MBRs, should be taken into account during operation. Increasing pressure when a membrane is fouled to maintain a constant flux may lead to compaction of the cake layer. Given that fouling layer compressibility may well influence filtration performance, it may be possible to improve MBR filtration by controlling fouling layer compressibility, e.g. by the addition of fine particles or changes in operating conditions to modify the cake structure [8]. For such studies, real-time monitoring techniques are essential for obtaining accurate information regarding the degree and reversibility of fouling layer compression. The present methodology shows this potential, but requires further development for adaption at the higher sludge concentrations typical of MBRs.

4. Conclusions

This study demonstrates the value of employing a comprehensive methodology to assess the compressibility of fouling layers formed by activated sludge filtration. From time-series filtrations and post-mortem characterization of fouled membranes, it was determined that diluted activated sludge fouling of membranes decreased the ultrasonic reflected signal amplitude. However, monitoring of activated municipal sludge fouling at different pressures revealed that the fouling layers formed at higher pressure evidenced less ultrasonic amplitude reduction as compared to that at lower pressure. This is likely a consequence of fouling cake compression, as a denser and less water-swollen cake provides a less ultrasonically attenuating layer. This tendency was confirmed by similar observations in stepped-pressure experiments that incorporated systematic variations in pressure between the levels used in constant-pressure filtrations and by determination of a pressure-dependent fouling-layer resistance. By applying the pressure-step methodology, it may be possible to

monitor the fouling layer response for pressure changes under realistic conditions, both in terms of cake compression and cake swelling.

This study indicates that UR combined with a pressure-step filtration approach can be utilized for real-time characterization of the development and compression of fouling layers. UR can, thus, serve as an important tool to study strategies to limit permeability loss due to cake compression. However, further development of the methodology is necessary for successful adaption at the higher sludge concentrations typical for these systems.

Acknowledgments

The authors would like to acknowledge The Royal Danish Academy of Sciences and Letters, Niels Bohr Foundation, for financial support. Furthermore, Boulder Wastewater Treatment Facility is acknowledged for providing sludge for the experiments, and the Membrane Science, Engineering and Technology (MAST) Center at the University of Colorado Boulder is acknowledged for the use of ultrasonic instrumentation. We also thank Professor Mark Borden at University of Colorado Boulder for providing PSD measurement equipment and Lisbeth Wybrandt from Aalborg University for carrying out a portion of the EPS analysis.

References

[1] A. Drews, Membrane fouling in membrane bioreactors: Characterisation, contradictions, cause and cures, J. Membr. Sci. 363 (2010) 1–28.
[2] P. Le-Clech, V. Chen, T.A.G. Fane, Fouling in membrane bioreactors used in wastewater treatment, J. Membr. Sci. 284 (2006) 17–53.
[3] F. Meng, S.R. Chae, A. Drews, M. Kraume, H.S. Shin, F. Yang, Recent advances in membrane bioreactors (MBRs): Membrane fouling and membrane material, Water Res. 43 (2009) 1489–1512.
[4] Z. Wang, Z. Wu, A Review of membrane fouling in MBRs: Characteristics and role of sludge cake formed on membrane surfaces, Sep. Sci. Technol. 44 (2009) 3571–3596.
[5] M.L Christensen, The Effect of Filter Cake Viscoelasticity on Filtration: A Study of Activated Sludge Dewatering, PhD thesis, Aalborg University, Department of Biotechnology, Chemistry and Environmental Engineering, Aalborg, Denmark, 2006.
[6] M.L. Christensen, T.B. Nielsen, M.B.O. Andersen, K. Keiding, Effect of water-swollen organic materials on crossflow filtration performance, J. Membr. Sci. 333 (2009) 94–99.
[7] B.L. Sørensen, P.B. Sorensen, Applying cake filtration theory on membrane filtration data, Water Res. 31 (1997) 665–670.
[8] B. Teychene, C. Guigui, C. Cabassud, Engineering of an MBR supernatant fouling layer by fine particles addition: A possible way to control cake compressibility, Wat. Res. 45 (2011) 2060–2072.
[9] J. Zhang, H.C. Chua, J. Zhou, A.G. Fane, Factors affecting the membrane performance in submerged membrane bioreactors, J. Membr. Sci. 284 (2006) 54–66.
[10] E. Giraldo, M. LeChevallier, Dynamic mathematical modeling of membrane fouling in submerged membrane bioreactors, Proc. Water Environ. Fed. WEFTEC (2006) 4895–4913.
[11] X.-Y. Li, X.-M. Wang, Modelling of membrane fouling in a submerged membrane bioreactor, J. Membr. Sci. 278 (2006) 151–161.
[12] M.K. Jørgensen, T.V. Bugge, M.L. Christensen, K. Keiding, Modeling approach to determine cake buildup and compression in a high-shear membrane bioreactor, J. Membr. Sci. 409–410 (2012) 335–345.
[13] T.V. Bugge, M.K. Jørgensen, M.L. Christensen, K. Keiding, Modeling cake buildup under TMP-step filtration in a membrane bioreactor: Cake compressibility is significant, Water Res. 46 (2012) 4330–4338.
[14] V. Chen, H. Li, A.G. Fane, Non-invasive observation of synthetic membrane processes—A review of methods, J. Membr. Sci. 241 (2004) 23–44.
[15] X.Y. Lu, E. Kujundzic, G. Mizrahi, J. Wang, K. Cobry, M. Peterson, J. Gilron, A. Greenberg, Ultrasonic sensor control of flow reversal in RO desalination—Part 1: Mitigation of calcium sulfate scaling, J. Membr Sci. 419–420 (2012) 20–32.
[16] X.H. Li, J.X. Li, J. Wang, H.W. Zhang, Y.D. Pan, In situ investigation of fouling behavior in submerged hollow fiber membrane module under sub-critical flux operation via ultrasonic time domain reflectometry, J. Membr. Sci. 411–412 (2012) 137–145.
[17] E. Kujundzic, A.R. Greenberg, R. Fong, B. Moore, D. Kujundzic, M. Hernandez, Biofouling potential of industrial fermentation broth components during microfiltration, J. Membr. Sci. 349 (2010) 44–55.
[18] E. Kujundzic, A. Cristina Fonseca, E.A. Evans, M. Peterson, A.R. Greenberg, M. Hernandez, Ultrasonic monitoring of earlystage biofilm growth on polymeric surfaces, J. Microbiol. Methods 68 (2007) 458–467.
[19] S.K. Sikder, M.B. Mbanjwa, D.A. Keuler, D.S. McLachlan, F.J. Reineke, R.D. Sanderson, Visualisation of fouling during microfiltration of natural brown water by using wavelets of ultrasonic spectra, J. Membr. Sci. 271 (2006) 125–139.
[20] J.-X. Liu, J.-X. Li, X.-M. Chen, Y.Z. Zhang, Monitoring of polymeric membrane fouling in hollow fiber module using ultrasonic nondestructive testing, Trans. Nonferrous Met. Soc. China 16 (2006) s845–s848.
[21] X. Xu, J. Li, N. Xu, Y. Hou, J. Lin, Visualization of fouling and diffusion behaviors during hollow fiber microfiltration of oily wastewater by ultrasonic reflectometry and wavelet analysis, J. Membr. Sci. 341 (2009) 195–202.
[22] E. Kujundzic, A.R. Greenberg, M. Peterson, Ultrasonic characterization of membranes, Desalin. Water Treat. 52 (2014) 1217–1249.
[23] B. Frølund, R. Palmgren, K. Keiding, P.H. Nielsen, Extraction of extracellular polymers from activated sludge using a cation exchange resin, Water Res. 30 (1996) 1749–1758.

[24] O.H. Lowry, N.J. Rosebrough, A.L. Farr, R.J. Randall, Protein measurement with the folin phenol reagent, J. Biol. Chem. 193 (1951) 265–275.
[25] K. Raunkjær, T. Hvitved-Jacobsen, P.H. Nielsen, Measurement of pools of protein, carbohydrate and lipid in domestic wastewater, Water Res. 28 (1994) 251–262.
[26] A.F. Gaudy, Colorimetric determination of protein and carbohydrate, Indust. Water Wastes 7 (1962) 17–22.
[27] R.A. Peterson, A.R. Greenberg, L.J. Bond, W.B. Krantz, Use of ultrasonic TDR for real-time noninvasive measurement of compressive strain during membrane compaction, Desalination 116 (1998) 115–122.
[28] D.C. Montgomery, G.C. Runger, Applied Statistics and Probability for Engineers, fourth ed., Wiley, New York, NY, 2007.
[29] A.P. Mairal, A.R. Greenberg, W.B. Krantz, L.J. Bond, Real-time measurement of inorganic fouling of RO desalination membranes using ultrasonic time-domain reflectometry, J. Membr. Sci. 159 (1999) 185–196.
[30] A.P. Mairal, A.R. Greenberg, W.B. Krantz, Investigation of membrane fouling and cleaning using ultrasonic time-domain reflectometry, Desalination 130 (2000) 45–60.
[31] W.B. Krantz, A.R. Greenberg, Use of UTDR for Membrane Characterization, Advanced Membrane Technology and Applications, in: N. Li, A.G. Fane, W.S. Winston Ho, T. Matsuura (Eds.), Advanced Membrane Technology and Applications, Wiley, Hoboken, NJ, 2008, pp. 779–896.
[32] M.K. Jørgensen, K. Keiding, M.L. Christensen, On the reversibility of cake buildup and compression in a membrane bioreactor, J. Membr. Sci. 455 (2014) 152–161.
[33] G.Y. Chai, B. Cao, G.Y. Zhao, A.R. Greenberg, W.B. Krantz, Effects of concentration polarization, temperature and pressure on ultrasound detection of inorganic fouling and cleaning in a spiral-wound membrane module, Desalin. Water Treat. 50 (2012) 411–422.